Available online at www.sciencedirect.com

ScienceDirect

journal homepage: www.elsevier.com/locate/he

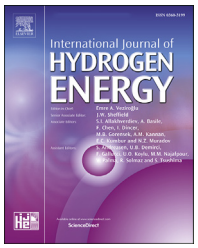

Valorization of the waste heat given off in a system alkaline electrolyzer-photovoltaic array to improve hydrogen production performance: Case study Antofagasta, Chile

Diego Contreras Bilbao

Facultad de Ingeniería, Universidad de Concepción, Chile

HIGHLIGHTS

- An annual simulation of a system alkaline electrolyzer-PV array is carried out.
- The waste heat given off by the electrolyzer is quantified and valorized.
- Waste heat is used to operate the electrolyzer continuously at its rated temperature.
- Annual hydrogen production increases by 0.22% and electrolyzer efficiency by 0.33%.
- Waste heat increases overall system efficiency by 13%.

ARTICLE INFO

Article history:
Received 6 March 2021
Received in revised form
5 June 2021
Accepted 4 July 2021
Available online 4 August 2021

Keywords:
Hydrogen production
Alkaline electrolyzer
Waste heat
Photovoltaic solar energy
System simulation

ABSTRACT

The efficiency of an electrolyzer can be improved by preheating the water consumed, which is generally done by means of solar energy in PVT panels. In this research, the first objective is to determine whether it is possible to preheat the consumed water by using the residual heat given off by the electrolyzer itself fed by a PV array, and if the above is met, the second objective consists of quantify the benefits obtained in the performance of the system. The simulation is carried out over a period of one year, considering the meteorological conditions of the city of Antofagasta, Chile. The results indicate that it is possible to constantly maintain the water temperature consumed by the electrolyzer at its nominal value of 80 °C, since the energy contained in the waste heat is about 30 times higher than this hot water demand. Continuous operation at 80 °C compared to operation at variable temperature achieves an annual increase of 0.22% in hydrogen production and an average of 0.33% in electrolyzer efficiency. Moreover, by considering the thermal energy given off by the electrolyzer as useful output of the system, the overall energy efficiency increases by a relative percentage of 13%.

E-mail address: dcontrerasb@udec.cl.
https://doi.org/10.1016/j.ijhydene.2021.07.016

Nomenclature

Symbols

A	Electrode area (m^2)
AM	Air mass
A_{PV}	Photovoltaic array area (m^2)
C_{cw}	Thermal capacity of cooling water (J/K)
$C_{p,x}$	Specific heat on molar basis (J mol^{-1} K^{-1})
C_t	Overall thermal capacity of the electrolyzer (J/K)
E_x	Exergy (J)
F	Faraday constant; 96,485 C/mol
f_1	Parameter related to Faraday efficiency (A^2 m^{-4})
f_2	Parameter related to Faraday efficiency
G_{sc}	Solar constant, 1367 W/m^2
ΔG	Variation of Gibbs free energy (J/mol)
H_f°	Enthalpy of formation (J/mol)
ΔH	Enthalpy variation (J/mol)
I	Current (A)
I_b	Beam radiation (W/m^2)
I_a	Diffuse radiation (W/m^2)
I_{GH}	Global horizontal radiation (W/m^2)
I_T	Total incident radiation on an inclined surface (W/m^2)
$I_{o'}$	Radiation outside the atmosphere (W/m^2)
I_{ph}	Light-generated current (A)
I_0	Saturation current of a diode (A)
I_{mp}	Current at maximum power point (A)
I_{sc}	Short circuit current (A)
$K_{\tau\alpha}$	Incidence angle modifier
k_T	Clarity index
M	Air mass modifier
n	Correlative day of the year
N_s	Number of cells connected in series in a panel
N_{ss}	Number of panels connected in series
N_{pp}	Number of panels connected in parallel
$\dot{n}_{H_2}$	Hydrogen molar flux (mol/s)
$\dot{n}_{H_2O}$	Water molar flux (mol/s)
P_{ELT}	Electrolyzer power (W)
p	Electrolyzer operating pressure (bar)
p_{ref}	Reference pressure, 1 bar
R_b	Ratio between beam radiation on an inclined surface and the same on a horizontal surface
R_s	Panel series resistance (Ω)
R_p	Panel parallel resistance (Ω)
$r_{1,2}$	Parameter related to ohmic resistance of electrolyte (Ω m^2)
S	Radiation absorbed by the photovoltaic panel (W/m^2)
s	coefficient for overvoltage on electrodes (V)
S_f°	Entropy of formation (J mol^{-1} K^{-1})
ΔS	Entropy variation (J mol^{-1} K^{-1})
T	Electrolyzer operating temperature (°C)
T_a	Ambient temperature (°C o K)
$T_{cw,i}$	Water inlet temperature to the cooling system (°C)
$T_{cw,o}$	Cooling system water outlet temperature (°C)
T_c	Photovoltaic cell temperature (K)
T_{grid}	Temperature of the water supply network (°C)
T_{ref}	Reference temperature, 298 K
$t_{1,2,3}$	Coefficient for overvoltage on electrodes (A^{-1} m^2)
U	Electrolyzer operating voltage (V)
U_{rev}	Reversible voltage (V)
U_{rev}	Thermoneutral voltage (V)
UA_{HX}	Overall heat transfer coefficient-area product for heat exchanger (W/K)
V	Voltage (V)
V_{mp}	Voltage at maximum power point (V)
V_{oc}	Open-circuit voltage (V)
V_t	Diode thermal voltage (V)
z	Number of electrons transferred per reaction, 2

Greek symbols

$\alpha_{I_{sc}}$	Temperature coefficient of short circuit current (A/K)
$\beta_{V_{oc}}$	Temperature coefficient of open-circuit voltage (V/K)
β	Surface slope (°)
δ	Angle of declination (°)
η_F	Faraday efficiency
η_e	Energy efficiency of the electrolyzer
η_{ex}	Exergy efficiency
η_{PV}	Photovoltaic efficiency
$\eta_{S\to H_2}$	Sun to hydrogen efficiency
θ	Angle of incidence between beam radiation and the surface normal (°)
θ_z	Zenith angle (°)
θ_r	Angle of refraction (°)
ρ_g	Soil reflectivity
τ_t	Thermal time constant of the electrolyzer (s)
$\tau\alpha(\theta)$	Transmittance of the glazing system at one angleθ
φ	Latitude (°)
$\omega_{1,2}$	Hour angle (°)

Introduction

It is projected that in the next decades hydrogen will play a key role in the world energy system [1], providing a solution to the typical problems of renewable energies, such as their intermittency of generation and decoupling with the demand curve [2]. In the particular case of Chile, international organizations such as IEA [3] and Hydrogen Council [4] highlight it as one of the future major hydrogen producers in the world. The country has an abundant wind resource in the south and a great solar potential in the north [5], the latter being the largest in the world [6], making photovoltaic (PV) energy an ideal candidate for hydrogen production by means of electrolysis.

Although hydrogen production by means of an electrolyzer-PV system is attractive, the variability in solar radiation in the first and last hours of the day, causes the electrolyzer to work far from its nominal operating conditions, such as its temperature. Mraoui et al. [7] studied the direct coupling between a PV array and a PEM electrolyzer, and obtained an average difference of 7% for the RMSE between the

operating points calculated analytically and experimentally; justifying these results by the slow response time of the electrolyzer, mainly at sunrise and sunset; furthermore, the mathematical model of the electrolyzer did not take into account the influence of the cell temperature. Nguyen Duc et al. [8] also studied experimentally the optimization of the PV-electrolyzer coupling, and highlights the slow response time of the electrolyzer when it does not receive a preheating in the initial hours of the day, taking about 2 h to reach the nominal operating temperature of 60 °C. Finally, Rosa [9] experimentally determined a time of 2.5–3 h for an 8.5 kW alkaline electrolyzer to reach nominal operating conditions when powered by a PV array, compared to about 0.7 h when the system is powered by grid electricity.

This variability in the solar radiation causes the electrolyzer to work far from its nominal operation, which results in a drop in the nominal efficiency of the system. An alternative to improve the efficiency of the electrolyzer is to preheat the water used in electrolysis [10]. Working at higher temperatures increases the kinetics of the chemical reaction by decreasing the activation potential, in addition to improving the conductivity of the cells and decreasing the ohmic overpotential [11]; which finally leads to an increase in the efficiency of the electrolyzer due to a decrease in the specific energy consumption [12]. In the literature, it is possible to find different investigations in which electrolysis water is preheated by novel methods. For example, Wang et al. [13] used a photovoltaic-thermal PVT module to increase the PV efficiency and at the same time preheat the electrolysis water, obtaining a 4.2% decrease in the electricity consumed by the electrolyzer as a result of the latter. Oruc et al. [14] proposed a new architecture in which a PV module is integrated on top of an electrolyzer, using the waste heat from the module to preheat the electrolysis water. The developed model produced a nearly 2.5-fold increase in hydrogen production compared to a conventional electrolyzer operating at ambient temperature. Cilogluları et al. [15] also studied hydrogen production and domestic hot water generation using a PVT panel, showing that the increase in PV efficiency resulting from the cooling of the panel influences hydrogen production; however, the author does not quantify the benefits obtained with the new system implemented in comparison with a conventional PV-electrolyzer system. Yilmaz et al. [16] studied the production of hydrogen by means of a geothermal source, with which the electricity consumed by the electrolyzer is generated by an organic Rankine cycle. The residual geothermal water was used to preheat the water consumed by the electrolyzer, finding that the power required to generate 1 kg of hydrogen decreases by about 3%. The benefits of operating an electrolyzer at higher temperature are also quantified by Pino et al. [17], who used a wind turbine as an energy source. The author compared the performance of the electrolyzer operating under real conditions and under a constant nominal temperature assumption, finding that for the latter case the power consumption of the electrolyzer was between 1.2% and 9.4% lower compared to the experimental results.

In a commercial electrolyzer, the irreversibilities of the internal chemical reactions are expressed in the form of overpotentials or overvoltages, which tend to increase the voltage required in the electrolysis cells with respect to the theoretical minimum voltage [9]. This difference in voltages causes the generation of residual heat inside the electrolyzer, which must be removed by a cooling system in order not to exceed the nominal operating temperature [12]. In this theoretical research, the water consumed in the electrolysis will be preheated to improve the overall performance of a PV array-alkaline electrolyzer system; presenting as a novelty the use of the residual heat given off in the electrolyzer itself, which has not been studied according to the literature review. The waste heat is intended to increase the water temperature of the cooling system up to the nominal temperature of the electrolyzer used, which corresponds to 80 °C, then this hot water will be stored and used in the electrolysis process mainly in the hours of lower solar radiation. The first objective of this study is to determine if the waste heat from the electrolyzer can be used to preheat the electrolysis water to the nominal temperature value of 80 °C during the entire simulation period. If the first objective is met, the second objective is to make a comparison between the performance of the system operating under normal conditions (without using the waste heat) and the system operating at its nominal temperature due to the use of the waste heat. This comparison will be quantified in terms of hydrogen production and average efficiencies (energy and exergy) for both systems over a simulation period of 1 year. Due to the high levels of solar radiation that it has, and therefore greater potential for hydrogen generation, the city under study will be Antofagasta, Chile.

System description

Fig. 1 shows a general scheme of the studied system, where Fig. 1-(a) represents the base case and Fig. 1-(b) the proposed case. The base case is formed by a PV array that by means of a DC-DC converter with MPPT supplies electric power to the alkaline type electrolyzer. The electrolyzer consumes liquid water and decomposes it into hydrogen and oxygen in the gaseous phase. In order not to exceed the operating temperature of the electrolyzer, it has a cooling system, which consists of a heat exchanger that uses water from the supply network as the working fluid. The system shown in Fig. 1-(b) uses the same principle of operation as described above for the base case, only with the addition of a storage tank in which some of the high temperature water from the cooling system output is stored. The water stored in this tank will be consumed by the electrolyzer at times of the day when the power supplied by the PV array is not sufficient to reach the nominal operating temperature of the electrolyzer, which corresponds to 80 °C.

The study of systems involves the following constraints:

- Only hydrogen and oxygen production are considered, not considering the storage method.
- Although Fig. 1 shows a block corresponding to feedwater treatment, the design of this system is not considered; it is only included because of its importance in hydrogen generation.
- In the base case, no use is considered for the high temperature water from the heat exchanger. In the proposed case, if the amount of high temperature water from the

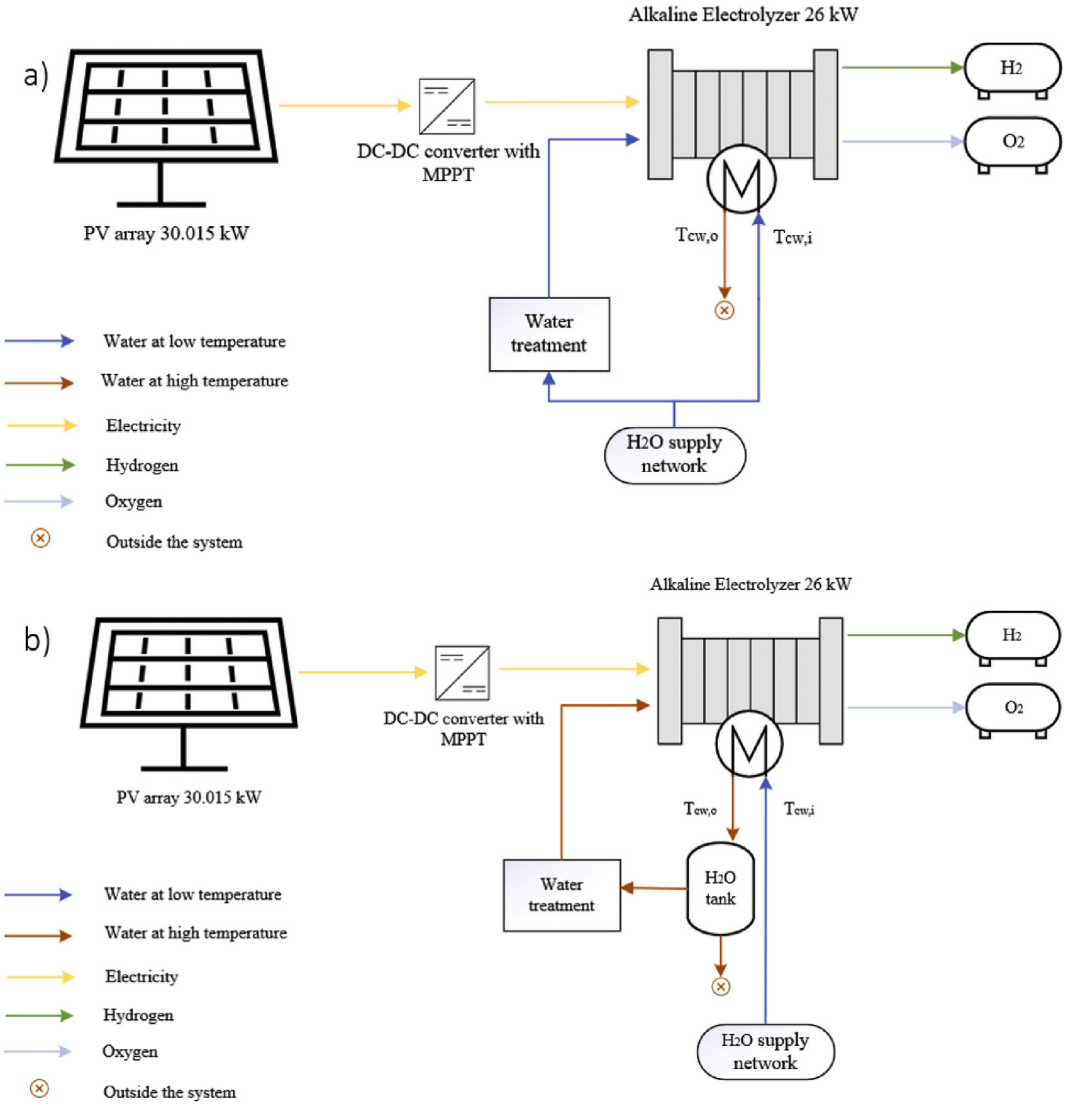

Fig. 1 – a) System used as base case, b) Proposed system.

heat exchanger is greater than the consumption demand of the electrolyzer, no use for this surplus is considered either.

The meteorological data are obtained on an hourly basis (see Section Available solar radiation), totaling 8760 simulation steps for the year of study. The simulation is performed in Matlab software.

Description of the electrolyzer model

For the mathematical modeling of the electrolyzer, the model proposed by Ulleberg [18] will be used. The electrolyzer studied by Ulleberg [18], which will be considered in the present investigation, uses as electrolyte a stationary solution of KOH at 30% by weight, operates at a pressure of 7 bar and a temperature of 80 °C, and has a rated power of 26 kW at 40 V.

The electrode kinetics of one electrolyzer cell can be modeled on the basis of a current-voltage (I–U) curve, which takes into account the temperature dependence of the overvoltages [18]:

$$U = U_{rev}(T) + \frac{r_1 + r_2 T}{A} I + s \log\left(\frac{t_1 + t_2/T + t_3/T^2}{A} I + 1\right) \quad (1)$$

Knowing the I-U curve, the electrical power of the electrolyzer P_{ELT} is calculated by multiplying these two terms, since it operates with direct current:

$$P_{ELT} = I\,U \quad (2)$$

The temperature of the electrolyte in the electrolyzer can be determined on the basis of a concentrated thermal capacitance model [18]:

$$T(\Delta t) = \left(T_{ini} - \frac{b}{a}\right)\exp(-a\Delta t) + \frac{b}{a} \quad (3)$$

The details of the implemented model, in addition to the

different constants and parameters used in Eqs. (1) and (3), is shown in Section D of the supplementary material.

Available solar radiation

Meteorological data

The meteorological information was extracted from the Dirección Meteorológica de Chile [19], using data from the Cerro Moreno Antofagasta Ap. station, which is located at a latitude of −23.453611° and a longitude of −70.445277°. From this station, horizontal global radiation, ambient temperature and wind speed at 10 m height were obtained on an hourly basis; all for the year 2018, being this period the most recent one published on the website. Fig. 2 shows the monthly horizontal global radiation and ambient temperature measured in 2018.

Radiation on inclined surfaces

To determine the total incident radiation on an inclined surface, the isotropic sky model [20] will be used:

$$I_T = I_b R_b + I_d\left(\frac{1+\cos\beta}{2}\right) + I_{GH}\rho_g\left(\frac{1-\cos\beta}{2}\right) \quad (4)$$

Representing the first term on the right the beam radiation, the second the isotropic diffuse radiation and the third the radiation reflected from the ground; while ρ_g indicates the ground reflectivity, a value that was assumed to be 0.2. R_b is the ratio between the beam radiation on an inclined surface and the same on a horizontal surface; that is, it is dependent on the angle of incidence θ between the direct radiation on a surface and the surface normal, and the zenith angle θ_z.

The clarity index k_T corresponds to the quotient between the global radiation I_{GH} and the extraterrestrial radiation I_o:

$$k_T = I_{GH}/I_o \quad (5)$$

where the extraterrestrial radiation on an hourly basis is obtained by the following relation [20]:

$$I_o = \frac{12\times 3600}{\pi} G_{sc}\left(1+0{,}033\cos\frac{360n}{365}\right)\left[\cos\phi\cos\delta(\sin\omega_2-\sin\omega_1) + \frac{\pi(\omega_2-\omega_1)}{180}\sin\phi\sin\delta\right] \quad (6)$$

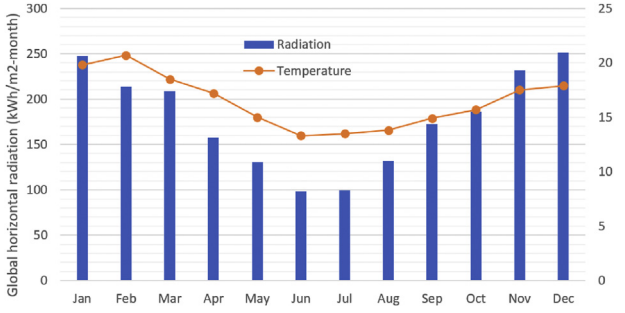

Fig. 2 – Global horizontal radiation and monthly mean ambient temperature, year 2018 [19].

The different terms presented in Eqs. (4)–(6) (R_b, G_{sc}, n, θ, ϕ, δ, θ_z and ω) are calculated as explained in Chapter 1 of Duffie et al. [20], and for simplicity omits its development in the present study. Once the clarity index k_T is known, the diffuse radiation I_d is obtained by means of Orgill et al. [21] correlation.

Finally, the orientation of the solar radiation capturing surface will have an azimuth value of 180° (taking as origin the south pole), while the inclination while the inclination will be 20°, in order to maximize the incident annual radiation [22].

Photovoltaic system model

The behavior of the photovoltaic system will be developed based on a 5-parameter model, which are determined according to the method proposed by Ma et al. [23]. In the first instance the 5 parameters are obtained in standard test conditions STC, then they are calculated in general operating conditions, taking into consideration factors such as cell temperature, angle of incidence of solar radiation, air mass, among others. The detailed modeling of the PV system is shown in Section B of the supplementary material.

The coupling of the PV-electrolyzer system will be done by means of a DC-DC device, which adapts the voltage output of the PV array according to the required input of the electrolyzer, in addition to guaranteeing the operation of the PV field at its MPP, thus maximizing hydrogen production [24]. The DC-DC converter includes a "maximum power point tracking" (MPPT) system, therefore, an algorithm must be found that calculates the MPP for each hour of the simulated year, according to the different existing weather conditions. The algorithm developed in this research is presented in Section C of the supplementary material. In the calculations performed, the DC-DC converter has been considered to have a constant efficiency of 95% [25].

Finally, the photovoltaic panels simulated in this study have a nominal power of 133.4 W and are of the single-crystalline type, whose main characteristics are shown in Table A.3 of the supplementary material. A total of 225 panels will be connected, totaling a nominal power of 30.015 kW.

Available thermal energy

As mentioned above, the cooling system of the electrolyzer is intended to decrease the operating temperature when the operating temperature exceeds the nominal value of 80 °C. The operating temperature of the electrolyzer within a certain time interval can be determined by means of Eq. (3). If in the calculations performed the operating temperature T exceeds 80 °C, then for each time interval considered the cooling system should be able to extract the following amount of thermal energy:

$$\varepsilon_{HX} C_t (T - 80\,^\circ\mathrm{C}) = C_{cw}\left(T_{cw,o} - T_{cw,i}\right) \quad (7)$$

where C_t and C_{cw} are respectively the heat capacities of the electrolyzer and the cooling water flow rate, and ε_{HX} is the heat exchanger efficiency, which was assumed to be 0.7 [26]. $T_{cw,o}$ and $T_{cw,i}$ represent the outlet and inlet temperature of the cooling water to the heat exchanger, the latter being obtained

from Ref. [27]. Eq. (7) is used to determine the value of C_{cw}, which represents the product between the specific heat of the water and the mass flow necessary to lower the temperature of the electrolyzer to 80 °C. The water temperature at the exchanger outlet $T_{cw,o}$ will be set at 90 °C, which will be partly stored to be later consumed by the electrolyzer during periods of low solar radiation, when the nominal value of 80 °C is not reached. The temperature of the stored water was oversized by 10 °C to take into account the thermal losses to the surroundings, which, together with the volume of the storage tank, will not be calculated in this study.

Furthermore, the heat exchanger is considered with a sufficient area to reach the desired temperatures of 80 °C in the electrolyzer and 90 °C for $T_{cw,o}$. The calculations also take into account the restriction imposed by thermodynamic laws regarding the maximum possible heat transfer [28]:

$$\dot{Q}_{max} = C_{min}\left(T - T_{cw,i}\right) \tag{8}$$

where C_{min} represents the minimum heat capacity ratio between that of the electrolyzer and that of the cooling water. The term in parentheses corresponds to the maximum temperature difference that can occur in the heat exchanger.

System performances

The energy efficiency of the PV array, of the electrolyzer and of Sol to hydrogen will be calculated respectively by Eqs. (9)–(11):

$$\eta_{e,PV} = \frac{P_{MPPT}\ \eta_{DC-DC}}{I_T A_{PV}} \tag{9}$$

$$\eta_{e,ELT} = \frac{\dot{m}_{H_2} HHV_{H_2}}{P_{MPPT}\ \eta_{DC-DC}} \tag{10}$$

$$\eta_{e,S\to H_2} = \frac{\dot{m}_{H_2} HV_{H_2}}{I_T A_{PV}} \tag{11}$$

where P_{MPPT} is the power in the photovoltaic MPP, η_{DC-DC} the efficiency of the converter, $\dot{m}_{H_2}$ is the mass flow rate of hydrogen produced and HHV_{H_2} is the higher heating value of hydrogen, assumed ass 141 MJ/kg [29].

Analogously to the energy analysis presented, the exergy efficiency will be calculated by means of Eqs. (12)–(14):

$$\eta_{ex,PV} = \frac{P_{MPPT}\ \eta_{DC-DC}}{Ex_{Sun}} \tag{12}$$

$$\eta_{ex,ELT} = \frac{\dot{n}_{H_2} Ex_{H_2}}{P_{MPPT}\ \eta_{DC-DC}} \tag{13}$$

$$\eta_{ex,S\to H_2} = \frac{\dot{n}_{H_2} Ex_{H_2}}{Ex_{Sun}} \tag{14}$$

where $\dot{n}_{H_2}$ is the molar hydrogen production and Ex_{H_2} is the chemical exergy of hydrogen, which has a value of 2.352×10^5 J/mol [13]. Ex_{Sun} is the solar energy exergy input rate [30]:

$$Ex_{Sun} = \left[1 - \frac{4}{3}\frac{T_a}{T_{Sun}} + \frac{1}{3}\left(\frac{T_a}{T_{Sun}}\right)^4\right] I_T A_{PV} \tag{15}$$

where the Sun's surface temperature T_{Sun} was assumed to be 5774 K [31]. Additionally, in the proposed case, the thermal energy released by the electrolyzer $\dot{Q}_{ELT}$ is accounted for in the efficiency calculations. Once $\dot{Q}_{ELT}$ has been calculated using Eq. (7) in units of time, the global efficiency is calculated in energy and exergy terms:

$$\eta_{n,Global} = \frac{\dot{m}_{H_2} HHV_{H_2} + \dot{Q}_{ELT}}{I_T A_{PV}} \tag{16}$$

$$\eta_{ex,Global} = \frac{\dot{n}_{H_2} Ex_{H_2} + \dot{Q}_{ELT}\left(1 - \frac{T_a}{T}\right)}{Ex_{Sun}} \tag{17}$$

Results and discussion

Electrolyzer curves

As mentioned in Section Description of the electrolyzer model, the simulations performed correspond to the electrolyzer studied by Ulleberg [18], whose main operating parameters are shown in Table A.2 of the supplementary material. Based on these parameters, the current density-voltage curve for one cell of Eq. (1) was plotted for different temperatures. The curves obtained are shown in Fig. 3, where it can be seen that for the same current level, a lower voltage is required, which translates into an increase in the energy efficiency of the electrolyzer. Additionally, Fig. 3 shows a series of experimental points that have been adapted from Ulleberg [18], in order to validate the resolution of the implemented model.

Photovoltaic curves

The curves that define the behavior of the photovoltaic panel were obtained after following the flow diagram in Fig. B2 and using the electrical parameters shown in Table A.3; both are shown in the supplementary material. Fig. 4 shows the I–V curves obtained for different levels of radiation and cell temperature, in addition to the calculated maximum power points.

To validate the 5-parameter model of Ma et al. [23] and the model developed in the present investigation to obtain the MPPT (see Section C of the supplementary material), the relative percentage error between the 5 MPP points shown in Fig. 4 and the corresponding experimental values measured by Davis et al. [32] and cited by De Soto et al. [33] will be calculated. According to the descending order shown in Fig. 4, the errors obtained are 0.083%, 0.0094%, −3.95%, 3.22% and 0.76%; which are considered acceptable to validate the accuracy of the implemented model.

Base case simulation

This section shows the results obtained after performing the annual simulation of the PV array-electrolyzer system for the base case, i.e., without the use of the thermal energy extracted by the cooling system. Due to the characteristics of the electrolyzer used, the following restrictions were considered in the calculations:

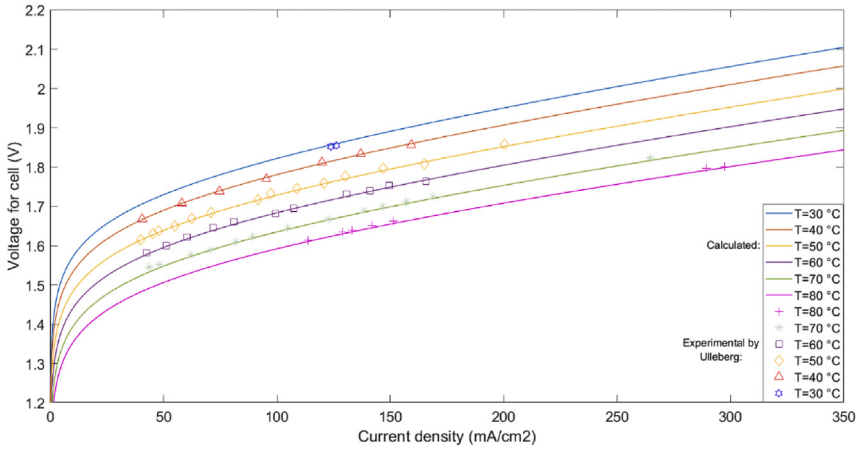

Fig. 3 – Current density-voltage curve for one electrolyzer cell calculated for different temperatures. The experimental points were adapted from Ulleberg [18].

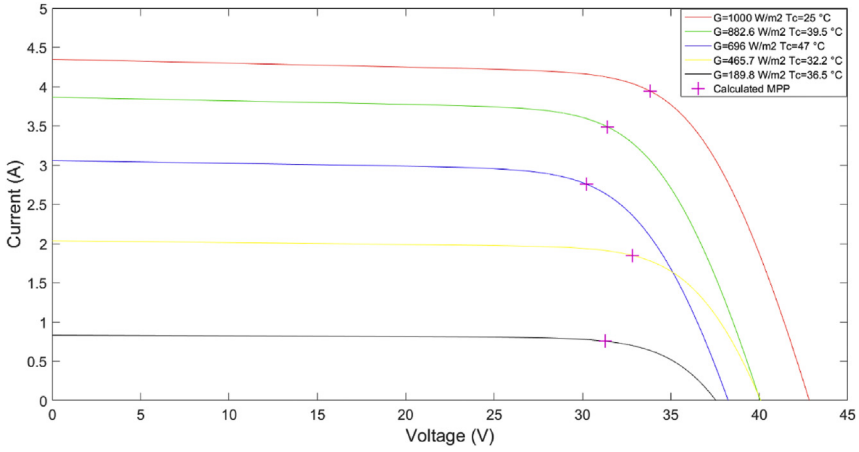

Fig. 4 – *I-V* curves for 133.4 W single-crystalline photovoltaic panel for different levels of radiation and cell temperature.

- The operating temperature must be less than or equal to 80 °C. If this value is exceeded, it is assumed that the cooling system is capable of regulating the temperature to the nominal value.
- Since the electrolyzer used is of the alkaline type, the hydrogen production starts when it reaches 20% of its rated power [18,34], i.e., 5200 W. In case the delivered power is greater than 100% of the electrolyzer capacity (26,000 W), it is assumed that the DC-DC converter is decoupled from the photovoltaic MPP in order not to deliver excess power to the electrolyzer.

Considering the above, a resolution algorithm has been developed in Matlab software, which is shown in Fig. 5. As input data, the algorithm requires the MPP power of the PV array, which is calculated according to Section C (supplementary material), and then multiplied by the efficiency of the DC-DC converter to finally obtain the power of the electrolyzer.

To obtain the current, voltage and operating temperature of the electrolyzer at each interval of 1 h during the year, it is necessary to solve a system composed of 3 nonlinear equations, for which the command 'fsolve' is used. When the operating temperature is equal to 80 °C, and since the power is also known, the current is obtained through Eq. (2), calculating the zeros of the function by means of the command 'fzero'.

Since the electrolyzer requires a power equal to 20% of its nominal capacity to start operating, there are intervals of the day in which there is solar radiation but no hydrogen production. For the simulated year, a total of 1053 h were counted in which this situation occurred. In order to illustrate the electrolyzer behavior, Fig. 6 shows the average daily operating power and temperature for different months of the year, as well as the total incident radiation on the PV array. It can be seen that in the months of higher radiation, the electrolyzer power reaches the nominal value of 26 kW in a greater number of hours during the day, which indicates that the DC-DC converter had to decouple from the PV MPP in order not to generate excess power in the electrolyzer. On the other hand, in the months of lower radiation, the excess power decreases, even being null in July. Alternatively, as an optimization method, the algorithm can be solved by varying the number of connected panels, in order to find a point

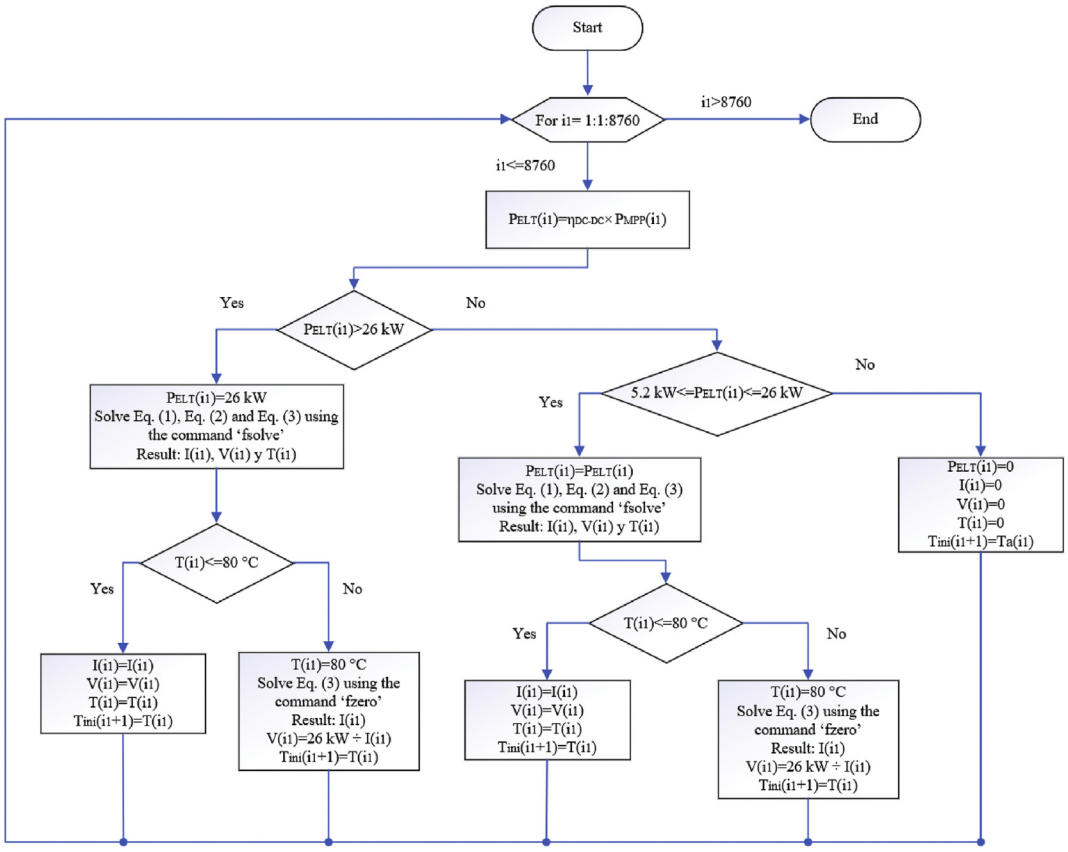

Fig. 5 – Algorithm developed in Matlab for the resolution of the base case.

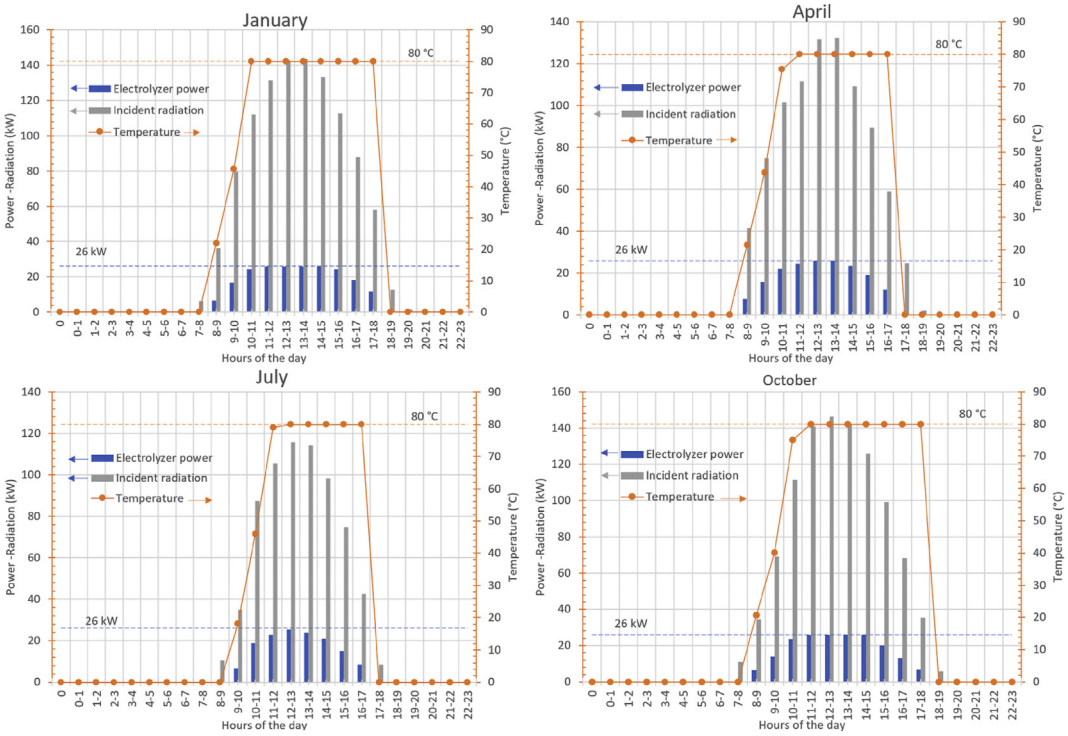

Fig. 6 – Incident radiation on PV array, power and operating temperature of the electrolyzer in hourly profiles for an average day of different months of the year, base case.

where the excess power and hydrogen production are balanced at a desired value.

The total hydrogen production for the different months of the year is shown in Fig. 7, where it can be seen that the highest production is obtained in the summer months, because this variable has a direct relationship with the current generated by the PV modules, which at the same time is a function of the available solar radiation. Fig. 7 also shows the average hours per day in which the electrolyzer operates, in addition to the average hours per day in which the electrolyzer is in operation, but at a temperature lower than 80 °C. It can be seen that on average for the year, of the total hours of daily operation of the electrolyzer only 70% does so at its nominal temperature.

Fig. 8 shows the different energy and exergy efficiencies calculated for the system. In the case of the photovoltaic panel, an improvement in efficiency is observed for the winter months due to a drop in the temperature of the cells, and it is also observed that the exergy efficiency is slightly higher than the energy efficiency, since it only considers the capacity to perform work from the incident solar radiation. The electrolyzer also shows a slight increase in efficiency in the winter months because it is operating at a lower current value, which decreases ohmic losses and reduces the overpotentials at the cathode and anode due to the lower bubbling rate in the gases [18]. Unlike the PV array, the energy efficiency of the electrolyzer is significantly higher than the exergy efficiency, due to the degradation of the consumed energy (thermal energy with high exergy value) into low quality thermal energy (low temperature water in the cooling system). Finally, the efficiency of Sol to hydrogen is mostly influenced by the low values presented by the PV efficiency, having an average of 13.25% for the energetic efficiency. It is also observed that the exergy efficiency presents a lower value compared to the energy efficiency, which is influenced by the energy degradation in the electrolyzer; however, the difference is not as marked as in the latter equipment due to the increase caused by the PV exergy efficiency.

When the operating temperature of the electrolyzer exceeds 80 °C, the cooling system is responsible for removing this excess thermal energy. Fig. 9 shows the amount of water used in the cooling system which, on average per day, can be heated from the grid temperature to 90 °C (the value is oversized to overcome thermal losses, as explained in Section Available thermal energy), after taking advantage of the thermal surplus of the electrolyzer. At the same time, Fig. 9 shows the average water consumption per day when the electrolyzer is in operation, but at a temperature lower than 80 °C. The two aforementioned values can be respectively assimilated as the average daily hot water supply and demand. According to the calculations made, it is important to note that in case of not using the cooling system, in a period of 1 h the operating temperature would increase from 80 °C to a maximum value close to 115 °C, taking as a reference a central hour of the day for the month of January, that is, when there is greater radiation. Due to the high heat capacity of the electrolyzer above that of the water, it is possible to increase the temperature of the latter to the desired value of 90 °C. As shown in Fig. 9, for all months of the year the hot water supply is much higher than the demand, even being 10 times higher in July and 50 times higher in January. This is explained by the low water consumption of the electrolyzer, which is less than 5 kg per hour even in the months with the highest radiation.

As a conclusion of the results obtained in Fig. 9, it is possible to use the heat captured by the cooling system to operate the electrolyzer continuously at a temperature of 80 °C, since the supply of hot water far exceeds the demand.

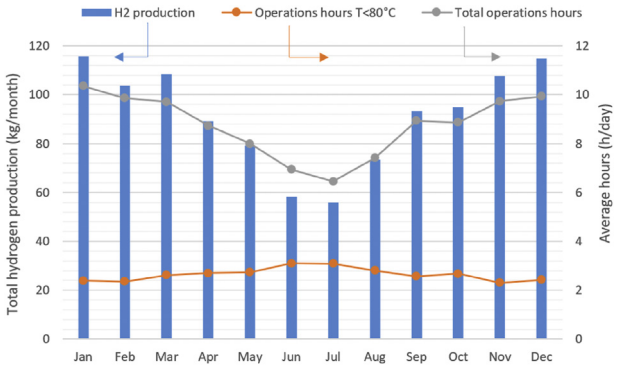

Fig. 7 – Total hydrogen production and operations hours, base case.

Proposed case simulation

Based on the results obtained in Section Base case simulation, in the proposed case it has been considered that the operating temperature has a constant value of 80 °C (an ideal cooling system is assumed), since the heat captured by the cooling system makes this situation possible. The solving algorithm used is shown in Fig. 10, which is run in Matlab. The electrolyzer power is identical to that of the base case, which depends on the PV array and the DC-DC converter, therefore the current can be obtained by Eq. (3) after applying the 'fzero' command, assuming a temperature of 80 °C.

Constantly maintaining the operating temperature at 80 °C resulted in a marginal increase in the performance indicators of the electrolyzer with respect to the base case, as shown in Fig. 11- (a). In absolute terms, annually the proposed case only increased hydrogen production by 2.4 kg over the base case, which represents a percentage increase of 0.22%. Increasing the operating temperature of the electrolyzer causes a decrease in the ohmic resistance, which implies that for a given current value there is a decrease in the cell voltage, as shown in Fig. 3. Therefore, for the same value of power consumed, the electrolyzer will operate at a higher current and a lower voltage compared to the same operation at a lower temperature. This explains the increase in the efficiency of the electrolyzer, which is close to 0.33%, as shown as a percentage in Fig. 11-(a). The slight increase in the efficiency of the electrolyzer causes the same effect on the Sun to hydrogen efficiency; while the photovoltaic efficiency remains constant, therefore it is not included in Fig. 11-(a). In addition, with the use of residual thermal energy it was not possible to increase the operating hours of the electrolyzer, maintaining the number of hours in which there is solar radiation but no hydrogen production at 1053 per year.

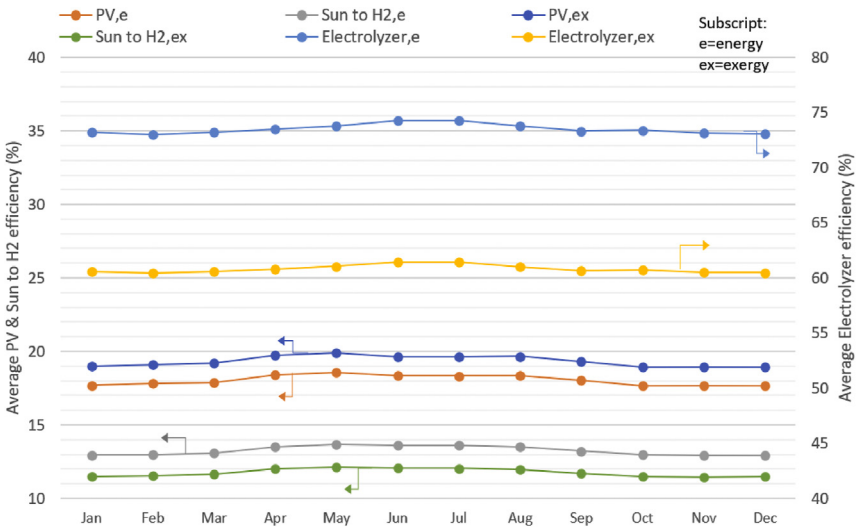

Fig. 8 – Monthly average energy and exergy efficiencies: electrolyzer, PV array and Sun to hydrogen; base case.

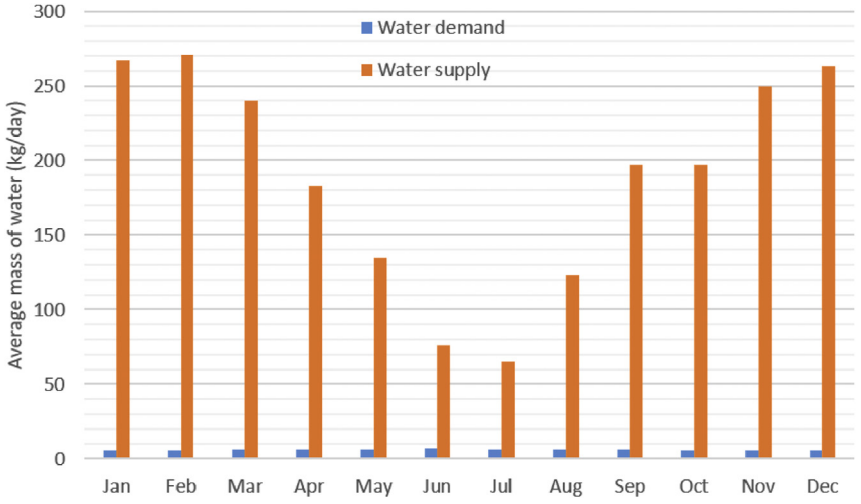

Fig. 9 – Average daily hot water supply and demand.

In the base case, the overall system performance is quantified by the Sun to hydrogen efficiency, which was shown in Fig. 8 and is repeated in Fig. 11-(b). For the proposed case, because the thermal energy gain is also considered as useful output, the performance is measured by the global efficiency, which is shown in Fig. 11-(b). In Fig. 11-(b) it can be seen that on average the global efficiency is 2 units higher than the efficiency of Sol to hydrogen, which corresponds to a relative percentage increase of 13%. Of the total useful energy in the proposed case, the thermal energy represents 11% and the energy contained in the hydrogen the remaining 89%. It can also be seen that the global efficiency presents a greater difference between the energetic and exergetic performance, due to the small capacity to generate work that water has at low temperature. In the winter months the amount of thermal energy contained in the waste heat decreases, therefore the global efficiency shows a drop in the months of June and July.

According to the results obtained, working constantly at 80 °C does not bring significant improvements in hydrogen production and system efficiencies. Although an increase in temperature benefits the performance of the electrolyzer, this does not become important in low-temperature electrolysis. For example, the reversible voltage and the thermoneutral voltage at 80 °C decrease respectively by 3.66% and 0.6% with respect to the same values at 20 °C. It should also be kept in mind that as shown in Fig. 7, during the year on average there are less than 3 h per day in which the electrolyzer operates at less than 80 °C. Finally, it is important to note that although an increase in temperature decreases the ohmic losses in the electrolyzer, it also increases the parasitic currents and consequently lowers the Faraday efficiency, thus affecting the total hydrogen production.

Comparison of results

The results of the present investigation show an improvement in system performance when operating constantly at the nominal electrolyzer temperature of 80 °C; however, this

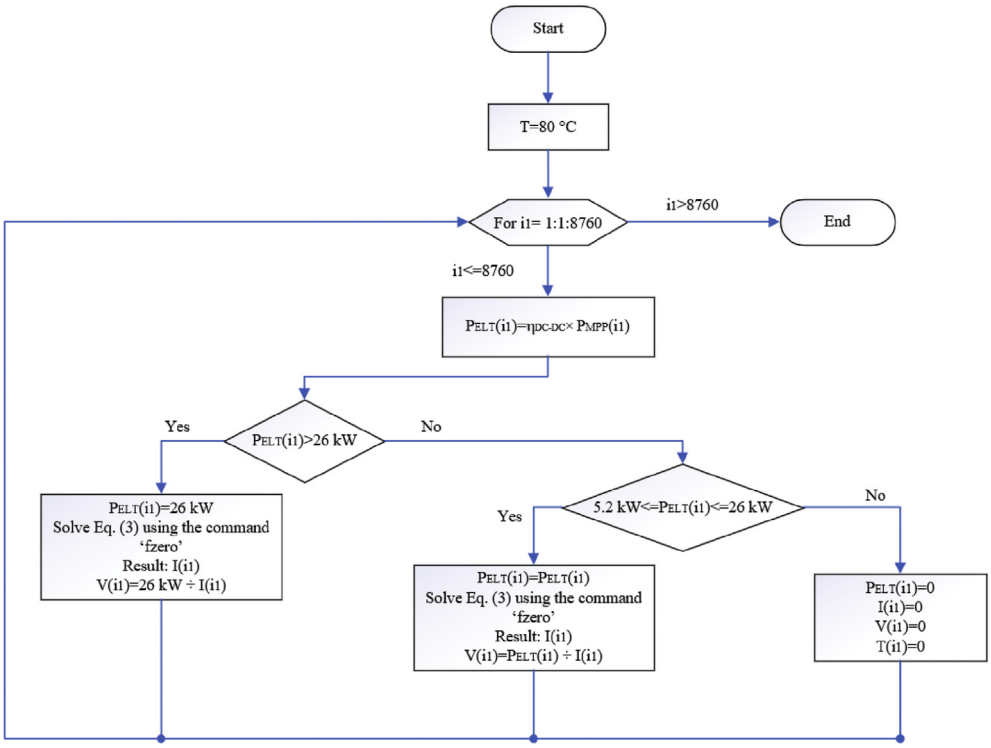

Fig. 10 – Algorithm developed in Matlab for the resolution of the proposed case.

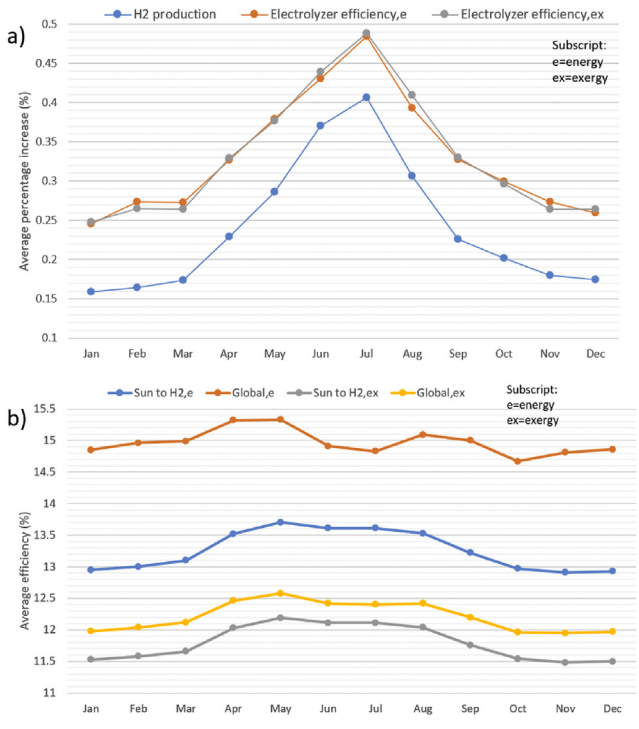

Fig. 11 – a) Percentage increase in the proposed case with respect to the base case: hydrogen production and efficiency of the electrolyzer. b) Global (proposed case) and Sol to hydrogen (base case) efficiency.

improvement is less than 5% in the different indicators analyzed, coinciding with the studies presented in Section Introduction. The calculated Sol to hydrogen efficiency of 13.5% is within the range of the literature (5.3% [35], 5.7% [9], 14.9% [8] and 17.29% [13]); however, it should be mentioned that some of these values are under special operating conditions and not annual averages.

In the literature reviewed, the preheating of the water consumed by the electrolyzer is generally performed by PVT solar panels, which has certain advantages and disadvantages compared to the proposed system. The first advantage is of the practical type, since PVT panels are not massively available on a commercial scale [36], which makes their implementation difficult. Furthermore as discussed in Refs. [13,14], the different operating conditions of the PVT panels present opposite benefits, since if the water flow to the electrolyzer is increased then the PV efficiency increases, but at the same time the water temperature decreases, which impairs the performance of the electrolyzer. However, as a point in favor of the PVT panels, it should be kept in mind that the influence of the PV efficiency is greater than that of the electrolyzer when analyzing the overall behavior of the system, as indicated by Ancona et al. [35], who attributes 89% of the total losses of the system to the conversion of solar energy to electrical energy. As an example of the above, the system proposed by Oruc et al. [14] increased hydrogen production by 2.5 times, however this benefit is mainly due to the increase in PV efficiency, and represents a particular case under defined operating conditions and not an annual average. Yilmaz et al. [16] obtained a 3% decrease in the specific energy consumption of the electrolyzer, however this value was also calculated under favorable operating conditions and does not represent an annual average.

It should also be noted that in the works [13–16] they use PEM type electrolyzers, the studies use PEM electrolyzers, which have a higher dynamic response compared to alkaline

Table 1 – Sensitivity analysis on hydrogen production for the base case and proposed case.

Simulation variables	Hydrogen production per year, base case (variable temperature)	Hydrogen production per year, proposed case (T = 80 °C)	Percentage increase proposed case respect base case (%)
Original simulation[a]	1.0945E3	1.097E3	0.27%
Nominal PV power			
23.345 kW	885.2286	887.7432	0.28%
16.675 kW	614.2601	616.8503	0.42%
Simulation step			
0.25 h	1.0912E3	1.0952E3	0.366%
Minimum electrolyzer capacity			
0%	1.1319E3	1.1354E3	0.3%

[a] PV power = 30.015 kW; Simulation step = 1 h; Minimum electrolyzer capacity = 20%.

electrolyzers, and are therefore preferable to use when integrated with fluctuating energy sources such as renewable energies. The difference between the mathematical modeling of the two electrolyzers could also influence the results obtained.

Sensitivity analysis

The previous sections have quantified the improvement in system performance when operating in the proposed case with respect to the base case. In order to extend the results obtained, this section will determine the variability of this improvement as a function of different input variables used in the simulation. The benefits will be quantified as a function of annual hydrogen production for the base case and the proposed case, and the different variables analyzed are as follows:

- Nominal power of the PV array: As the power of the photovoltaic array decreases, the number of hours in which it works below the nominal temperature increases, therefore the benefit obtained by working at constant temperature could be greater.
- Minimum capacity of the electrolyzer: If the electrolyzer were to start operating from a lower value in its input power, then there would be a greater number of periods in which it works below its nominal power, resulting in a situation similar to the one described in the previous point.
- Simulation steps: If the period used in the simulation steps is shorter, then the dynamic response of the electrolyzer is better captured, which could also influence the results.

The results are shown in Table 1, where the relative percentage increase in hydrogen production of the proposed case with respect to the base case is shown for the different simulation variables. If the latter term has a higher value, then under these simulation conditions it is more beneficial to work at constant temperature in the electrolyzer.

From the results presented in Table 1, it can be seen that the nominal power of the PV array is the variable that most influences the difference in hydrogen production between the proposed case and the base case. If the power delivered by the PV array is lower, then the electrolyzer operates away from its nominal conditions, therefore a higher benefit is obtained by constantly working at 80 °C. However, for all the variables analyzed, the improvement obtained by the proposed case is less than 1%, indicating a low influence of temperature on the system studied.

Conclusions

The present investigation sought to improve the performance of a PV-electrolyzer system by preheating the water consumed by using the waste heat given off by the electrolyzer itself. This energy is used to heat the cooling system water from the grid temperature to 90 °C, a value that is oversized with respect to the nominal electrolyzer temperature of 80 °C to account for thermal losses from the storage pond to the environment. This hot water is intended to be stored and subsequently consumed during the hours of the day when the electrolyzer operating temperature is below 80 °C. The first objective of the study is to determine whether it is possible to operate the electrolyzer continuously at the nominal value of 80 °C using this waste heat; then, as a second objective, a quantification of the benefits obtained in the performance of the system is carried out. The simulations were performed in steps of 1 h over one year, according to the meteorological conditions of the city of Antofagasta, Chile. The main conclusions obtained are shown below:

1) The mass of water available at 90 °C obtained after taking advantage of the heat transferred to the cooling system, on average for each day of the year is about 30 times higher than the water consumption of the electrolyzer in the hours in which it is in operation, but at a temperature lower than 80 °C. If the cooling system were not in operation, on the days with the highest radiation, the operating temperature would reach an average of 115 °C in the period of 1 h. Since the total heat capacity of the electrolyzer is higher than that of the water, it is possible to heat the latter up to 90 °C. It should also be considered that the water consumption in each hour, even for the months of higher radiation, is less than 5 kg, so there is a low demand for hot water compared to the amount that can be extracted from the cooling

system. In summary, by using the heat transferred to the cooling system, it is possible to work continuously at the nominal temperature of the electrolyzer of 80 °C.

2) The simulation compared the performance of the system working continuously at 80 °C (proposed case) and the system operating without the use of thermal energy (base case). For the period of one year, the proposed case had a total increase in hydrogen production of 0.22% over the base case, and the electrolyzer efficiency had average annual increase of 0.33%.
3) The change in hydrogen production of the proposed case with respect to the base case was subjected to a sensitivity analysis, finding that the capacity of the PV array is the most influential simulation variable, however, the difference between the results of the two cases has a marginal value of less than 1%, indicating the low influence of the operating temperature for the system studied.
4) Although the increase in the operating temperature of the electrolyzer brought improvements in hydrogen production and energy efficiency, these values are marginal. It was corroborated that increasing the operating temperature does not have a significant benefit on the electrolyzer performance, when the electrolysis is performed at low temperature. However, when considering the thermal energy contained in the waste heat of the electrolyzer, it represents 11% of the total useful energy output of the system, opening up a new field of application. In addition, the thermal energy results in a relative percentage increase of 13% in the overall efficiency.

The results obtained are valid under the operating parameters used. For example, due to the high levels of solar radiation present in the city of Antofagasta, the electrolyzer operates most of the time at its nominal temperature, which could be different if different meteorological conditions are considered. If another renewable source of greater variability is used, such as wind energy, the electrolyzer could operate below its nominal temperature at different periods of the day, and not only during sunrise as in the case studied. A situation similar to the one mentioned above can occur in facilities that store energy in the form of hydrogen and in batteries, where the electrolyzer also operates with multiple starts and stops. Finally, the great potential for using the waste heat given off by the electrolyzer in low-temperature applications, such as heat pumps or the preparation of domestic hot water, is highlighted.

Declaration of competing interest

The authors declare that they have no known competing financial interests or personal relationships that could have appeared to influence the work reported in this paper.

Acknowledgments

This work was funded by the National Agency for Research and Development (ANID); Scholarship Program/National Doctoral Scholarship/2020-21202256.

Appendix A. Supplementary data

Supplementary data to this article can be found online at https://doi.org/10.1016/j.ijhydene.2021.07.016.

REFERENCES

[1] IRENA. Global Renewables Outlook. Energy transformation 2050. Abu Dhabi: International Renewable Energy Agency; 2020.
[2] González J. Energías renovables. Barcelona: Reverté S.A.; 2009.
[3] IEA. The Future of Hydrogen: seizing today's opportunities. Paris: International Energy Agency; 2019.
[4] HC. Path to hydrogen competitiveness: a cost perspective. Brussels: Hydrogen Council; 2020.
[5] Minenergía GIZ. Energías Renovables en Chile: el potential eólico, solar e hidroeléctrico de Arica a Chiloé. Santiago: Gobierno de Chile, Ministerio de Energía; 2014.
[6] Fresco P. El futuro de la energía en 100 preguntas. Madrid: Nowtilus; 2018.
[7] Mraoui A, Benyoucef B, Hassaine L. Experiment and simulation of electrolytic hydrogen production: case study of photovoltaic-electrolyzer direct connection. Int J Hydrogen Energy 2018;43(6):3441–50. https://doi.org/10.1016/j.ijhydene.2017.11.035.
[8] Nguyen Duc T, Goshome K, Endo N, Maeda T. Optimization strategy for high efficiency 20 kW-class direct coupled photovoltaic-electrolyzer system based on experiment data. Int J Hydrogen Energy 2019;44(49):26741–52. https://doi.org/10.1016/j.ijhydene.2019.07.056.
[9] Rosa M. Estudio teórico y experimental sobre la producción de hidrógeno electrolítico a partir de energía solar fotovoltaica: diseño, operación y evaluación de una planta piloto de producción de hidrógeno electrolítico de 1,2 Nm3 H2/h [PhD thesis]. Sevilla: Universidad de Sevilla; 2003.
[10] Creus A. Energías renovables. Barcelona: Ceysa; 2008.
[11] Rajeshwar K, McConnell R, Licht S. Solar hydrogen generation: toward a renewable energy future. New York: Springer; 2008.
[12] Zini G, Tartarini P. Solar hydrogen energy systems: science and technology for the hydrogen economy. New York: Springer; 2012.
[13] Wang H, Li W, Liu T, Liu X, Hu X. Thermodynamic analysis and optimization of photovoltaic/thermal hybrid hydrogen generation system based on complementary combination of photovoltaic cells and proton exchange membrane electrolyzer. Energy Convers Manag 2019;183:97–108. https://doi.org/10.1016/j.enconman.2018.12.106.
[14] Oruc ME, Desai AV, Kenis PJA, Nuzzo RG. Comprehensive energy analysis of a photovoltaic thermal water electrolyzer. Appl Energy 2016;164:294–302. https://doi.org/10.1016/j.apenergy.2015.11.078.
[15] Cilogulları M, Erden M, Karakilcik M, Dincer I. Investigation of hydrogen production performance of a photovoltaic and thermal system. Int J Hydrogen Energy 2017;42(4):2547–52. https://doi.org/10.1016/j.ijhydene.2016.10.118.
[16] Yilmaz C, Kanoglu M. Thermodynamic evaluation of geothermal energy powered hydrogen production by PEM water electrolysis. Energy 2014;69:592–602. https://doi.org/10.1016/j.energy.2014.03.054.
[17] Pino FJ, Valverde L, Rosa F. Influence of wind turbine power curve and electrolyzer operating temperature on hydrogen production in wind–hydrogen systems. J Power Sources

2011;196(9):4418–26. https://doi.org/10.1016/j.jpowsour.2010.10.060.
[18] Ulleberg Ø. Modeling of advanced alkaline electrolyzers: a system simulation approach. Int J Hydrogen Energy 2003;28(1):21–33. https://doi.org/10.1016/S0360-3199(02)00033-2.
[19] MeteoChile. Servicios Climáticos, Ficha de la Estación Chile: dirección Meteorológica de Chile. Dirección General de Aeronáutica Civil; 2020 [Available from, https://climatologia.meteochile.gob.cl/application/informacion/ficha-de-estacion/230001. November 25.
[20] Duffie J, Beckman W. Solar engineering of thermal processes. 4 ed. New Jersey: John Wiley & Sons; 2013.
[21] Orgill JF, Hollands KGT. Correlation equation for hourly diffuse radiation on a horizontal surface. Sol Energy 1977;19(4):357–9. https://doi.org/10.1016/0038-092X(77)90006-8.
[22] CDT. Diseño y Dimensionamiento de Sistemas Solares Fotovoltaicos Conectados a Red. Santiago de Chile: corporación de Desarrollo Tecnológico. Cámara Chilena de la Construcción; 2013.
[23] Ma T, Gu W, Shen L, Li M. An improved and comprehensive mathematical model for solar photovoltaic modules under real operating conditions. Sol Energy 2019;184:292–304. https://doi.org/10.1016/j.solener.2019.03.089.
[24] Djafour A, Matoug M, Bouras H, Bouchekima B, Aida MS, Azoui B. Photovoltaic-assisted alkaline water electrolysis: basic principles. Int J Hydrogen Energy 2011;36(6):4117–24. https://doi.org/10.1016/j.ijhydene.2010.09.099.
[25] Gibson T, Kelly N. Optimization of solar powered hydrogen production using photovoltaic electrolysis devices. Int J Hydrogen Energy 2008;33(21):5931–40. https://doi.org/10.1016/j.ijhydene.2008.05.106.
[26] Yang Z, Zhang G, Lin B. Performance evaluation and optimum analysis of a photovoltaic-driven electrolyzer system for hydrogen production. Int J Hydrogen Energy 2015;40(8):3170–9. https://doi.org/10.1016/j.ijhydene.2015.01.028.
[27] Minenergía. Norma Técnica que determina algoritmo para la verificación de la contribución solar mínima de los Sistemas Solares Térmicos acogidos a la franquicia tributaria de la Ley Nº 20.365. Santiago: Ministerio de Energía, Gobierno de Chile; 2010.
[28] Cengel Y, Ghajar A. Transferencia de Calor y masa. 4 ed. México: McGraw-Hill; 2011.
[29] Cengel Y, Boles M. Termodinámica. 7 ed. México: McGraw-Hill; 2011.
[30] Petela R. Exergy of heat radiation. J Heat Tran 1964;86(2):187–92. https://doi.org/10.1115/1.3687092.
[31] Chen H, Li G, Zhong Y, Wang Y, Cai B, Yang J, Badiei A, Zhang Y. Exergy analysis of a high concentration photovoltaic and thermal system for comprehensive use of heat and electricity. Energy 2021;225. https://doi.org/10.1016/j.energy.2021.120300.
[32] Davis MW, Fanney AH, Dougherty BP. Evaluating building integrated photovoltaic performance models. Conference record of the twenty-ninth IEEE photovoltaic specialists conference, 20022002. p. 1642-1645.
[33] De Soto W, Klein SA, Beckman WA. Improvement and validation of a model for photovoltaic array performance. Sol Energy 2006;80(1):78–88. https://doi.org/10.1016/j.solener.2005.06.010.
[34] Gallardo FI, Monforti Ferrario A, Lamagna M, Bocci E, Astiaso Garcia D, Baeza-Jeria TE. A Techno-Economic Analysis of solar hydrogen production by electrolysis in the north of Chile and the case of exportation from Atacama Desert to Japan. Int J Hydrogen Energy 2021;46(26):13709–28. https://doi.org/10.1016/j.ijhydene.2020.07.050. ISSN 0360-3199.
[35] Ancona MA, Bianchi M, Branchini L, De Pascale A, Melino F, Peretto A, Rosati J, Scarponi LB. From solar to hydrogen: preliminary experimental investigation on a small scale facility. Int J Hydrogen Energy 2017;42(33):20979–93. https://doi.org/10.1016/j.ijhydene.2017.06.141.
[36] Herez A, El Hage H, Lemenand T, Ramadan M, Khaled M. Review on photovoltaic/thermal hybrid solar collectors: classifications, applications and new systems. Sol Energy 2020;207:1321–47. https://doi.org/10.1016/j.solener.2020.07.062.